Stochastic Modeling Hysteresis and Resistive Switching in Bipolar Oxide-Based Memory

Alexander Makarov, Viktor Sverdlov, and Siegfried Selberherr
Institute for Microelectronics, TU Wien
Wien, Austria
{makarov | sverdlov | selberherr}@iue.tuwien.ac.at

***Abstract*—We have developed a stochastic model of the resistive switching mechanism in resistive random access memory (RRAM) based on electron hopping. The distribution of electron occupation probabilities obtained with our approach is in good agreement with previous work. In particular, a low occupation region is formed near the cathode for bipolar switching behavior or near the anode for unipolar switching behavior. This result indicates that a decrease of the switching time with increasing temperature cannot be explained only by reduced occupations of the vacancies in the low occupation region, but is related to an increase of the mobility of the oxide ions. A hysteresis cycle of RRAM switching simulated with our stochastic model is in good agreement with experimental results.**

Keywords-RRAM; resistive switching mechanism; stochastic model; Monte Carlo method.

I. INTRODUCTION

Memory based on charge storage (such as flash memory, and others) is gradually approaching the physical limits of scalability. The increasing demand for minimization of microelectronic devises (e.g. MP3 players, mobile phones) has significantly accelerated the search for new concepts of nonvolatile memory during the last few years. Apart from good scalability a new type of memory must also exhibit low operating voltages, low power consumption, high operation speed, long retention time, high endurance, and simple structure [1], [2].

Several concepts as potential replacements of the charge memory were invented and developed. Some of the technologies are already available as prototype (such as carbon nanotube RAM (NRAM), copper bridge RAM (CBRAM)), others as product (phase change RAM (PCRAM), magnetoresistive RAM (MRAM), ferroelectric RAM (FRAM)), while the technologies of spin-torque transfer RAM (STTRAM), racetrack memory, and resistive RAM (RRAM) are under intensive research.

From these concepts the CBRAM, PCRAM, and RRAM possess the simplest structure in the form of metal–insulator–metal (MIM). The electrical conductance of the insulator can be set at different levels by the application of an electric field. In CBRAM, PCRAM, and RRAM different types of materials are used. CBRAM is based on solid state electrolyte in which mobile metal ions may create a conductive bridge between the two electrodes under the influence of an electric field. PCRAM employs the difference in resistivity between crystalline and amorphous phases of a chalcogenide compound. RRAM is based on metal oxides, such as TiO_x [3-6], HfO_2 [7], Cu_xO [8], NiO [9], ZnO [10] and perovskite oxides, such as doped $SrTiO_3$ [11], doped $SrZrO_3$ [12], $Pr_{1-x}Ca_xMnO_3$ [13].

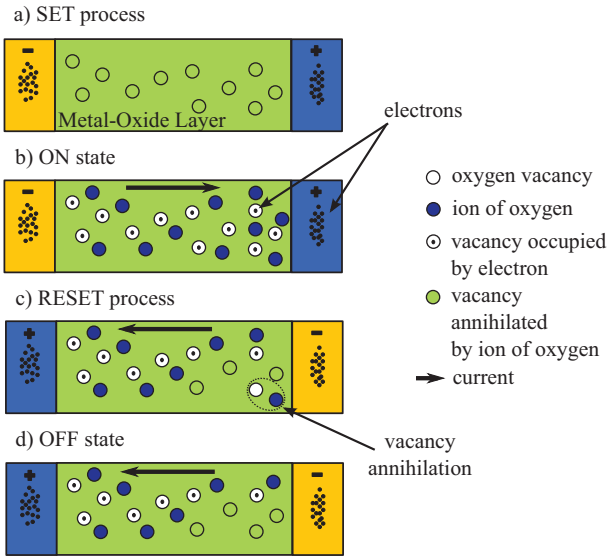

Figure 1. Illustration of the resistive switching mechanism in bipolar oxide-based memory cell: (a) Schematic illustration of the SET process. (b) Schematic view of the conducting filament in the low resistance state (ON state). (c) Schematic illustration of the RESET process. (d) Schematic view of the conducting filament in the high resistance state (OFF state). Only the oxygen vacancies and ions which impact the resistive switching are shown.

In addition to its simple structure RRAM is characterized by low operating voltage (<2V), fast switching time (<10 ns), high density, and long retention time.

Several physical mechanisms based on either electron or ion switching have been recently suggested in the literature: a model based on trapping of charge carriers [14], electrochemical migration of oxygen vacancies [15], [16], electrochemical migration of oxygen ions [17], [18], a unified physical model [19], a domain model [20], a filament anodization model [21], a thermal dissolution model [22], a two-variable resistor model [23], and others. Despite this, a proper fundamental understanding of the RRAM switching mechanism is still missing hindering further development of this type of memory.

This research is supported by the European Research Council through the grant #247056 MOSILSPIN.

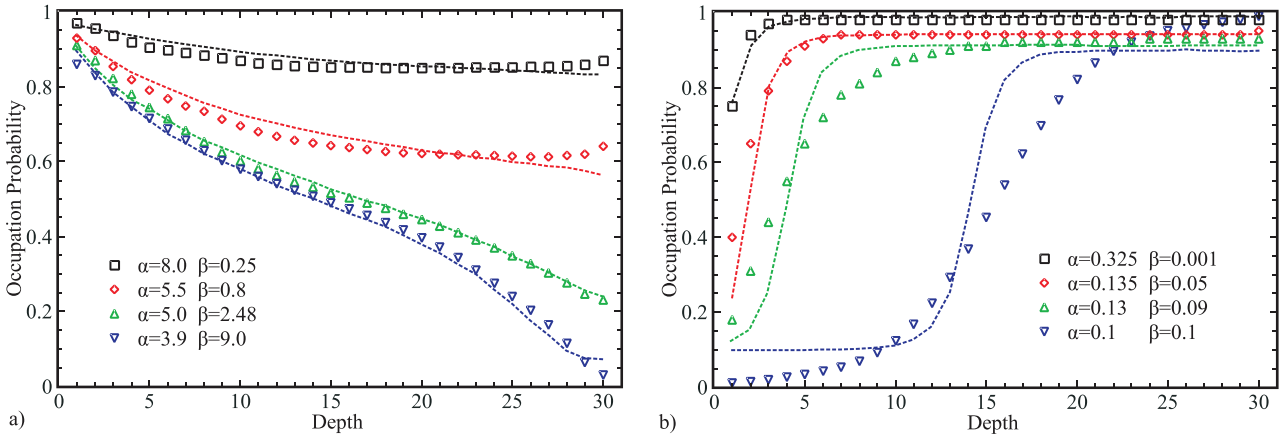

Figure 2. Calculated distribution of electron occupation probabilities under different biasing voltages. Lines are from [19], symbols are obtained from our stochastic model.

In this work we present a stochastic model of the resistive switching mechanism based on electron hopping between the oxygen vacancies along the conductive filament in an oxide-layer.

II. Model Description

We associate the resistive switching behavior in the oxide-based memory with the formation and rupture of a conductive filament (CF). The CF is formed by localized oxygen vacancies (V_o) [19] or domains of V_o. Formation and rupture of a CF is due to a redox reaction in the oxide layer under a voltage bias. The conduction is due to electron hopping between these V_o. (Fig. 1)

If the CF is formed, the following events can happen:

- an electron hop into V_o from an electrode;
- an electron hop from V_o to an electrode;
- an electron hop between two V_o.

In order to model the dependences of transport on the applied voltage and temperature we choose the hopping rates for electrons as [24]:

$$\Gamma_{nm} = A_e \cdot \frac{dE}{1-\exp(-dE/T)} \cdot \exp(-R_{nm}/a) \qquad (1)$$

Here, A_e is a coefficient, $dE=E_n-E_m$ is the difference between the energies of an electron positioned at sites n and m, R_{nm} is the hopping distance, a is the localization radius. The hopping rates between an electrode (0 or $N+1$) and an oxygen vacancy m are described [19]:

$$\Gamma_m^{iC} = \alpha \cdot \Gamma_{0m}, \Gamma_m^{oC} = \alpha \cdot \Gamma_{m0} \qquad (2)$$

$$\Gamma_m^{iA} = \beta \cdot \Gamma_{(N+1)m}, \Gamma_m^{oA} = \beta \cdot \Gamma_{m(N+1)} \qquad (3)$$

Here, α and β are the coefficients of the boundary conditions on the cathode and anode, respectively, N is the number of sites, A and C stand for cathode and anode, respectively, and i and o for hopping on the site and out from the site.

The current generated by hopping is calculated as:

$$I = q_e \cdot \sum dx / \sum \left(1 / \sum_m \Gamma_m \right) \qquad (4)$$

III. Model Verification

We first evaluate the average electron occupations of hopping sites under different conditions. For comparison with previous works all calculations of electron occupations of hopping sites are made on a one-dimension lattice consisting of thirty equivalent equidistantly positioned hopping sites V_o. All V_o are at the same energy level, if no voltage or temperature is applied. Despite the fact that in the binary metal oxides V_o can have three different charge states with charge 0, +1, +2, to simplify the calculations, we assume that the V_o is either empty or occupied by one electron.

At the initial moment of time we assume all sites to be empty. Electrons can hop from the cathode or anode positioned at 0 and $N+1$, respectively, provided the rate of this transition is nonzero. After the time interval t each site in the lattice will be either occupied by an electron or empty. In the following instance each electron will have a probability Γ_{nm} of hopping from the site n to the site m, provided the target site m is empty; moreover, an electron may enter the lattice at site m from the cathode with the probability $\alpha \cdot \Gamma_{0m}$ or from the anode with the probability $\beta \cdot \Gamma_{(N+1)m}$ (if this site m is empty) and an electron at site n may leave the lattice and hop to the cathode or the anode with the probability $\alpha \cdot \Gamma_{n0}$ or $\beta \cdot \Gamma_{n(N+1)}$, respectively.

We have calibrated the model in a manner to reproduce the results reported in [19], for V=0.4V to V=1.6V. Fig.2a shows a case, when the hopping rate between the electrodes and V_o is larger than the rate between the two V_o (i.e. α, β > 1). In this case the low occupation region is formed near the anode (unipolar behavior).

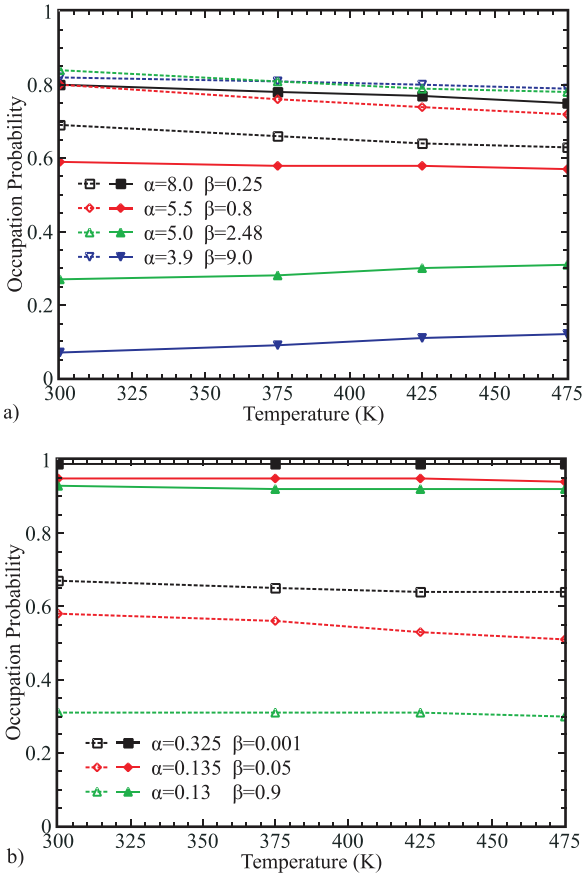

Figure 3. Temperature dependence of electron occupation probability near the anode (filled symbols) and the cathode (open symbols).

Fig.2b shows a case, when the hopping rate between the two V_o is larger than the rate between the electrodes and V_o (i.e. $\alpha, \beta < 1$). In this case a low occupation region is formed near the cathode (bipolar behavior).

The values of the coefficients of the boundary conditions are determined by the materials from which the electrode and the oxide-layer are made. A dependence of resistive switching on the electrode material was recently reported for ZrO_2 [25] and TiO_2 [26].

With the model calibrated in the manner described above we simulated the temperature dependence of the site occupations in the low occupation region. The results shown in Fig. 3a and Fig. 3b indicate high robustness of the low occupation region demonstrating changes of less than 10%, when the temperature is elevated from 25° *C* to 200° *C*. At the same time our finding indicates that the measured decrease of switching time with increasing temperature reported in [19] stems from the increased mobility of oxide ions rather than from reduced occupations of V_o in the low occupation region.

Results obtained from simulations of the temperature dependence of the site occupations in the low occupation region demonstrate the necessity to include the dynamics of oxygen ions.

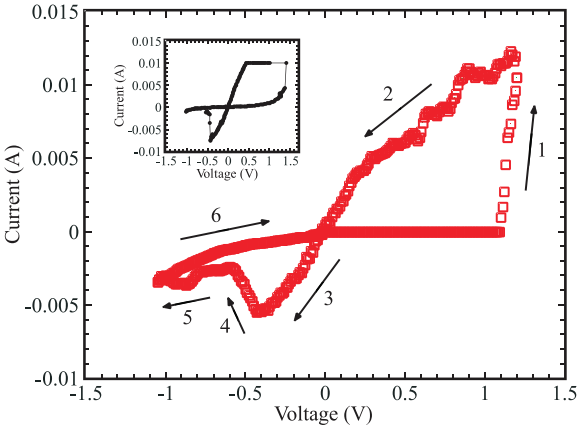

Figure 4. *I-V* characteristics showing the hysteresis cycle obtained from our stochastic model (α=0.1 and β=0.1). The inset shows the hysteresis cycle for *M*-ZnO-*M* from [10].

For modeling the resistive switching in oxide-based memory by Monte Carlo techniques, in addition to the possible events of moving an electron, described above, we handle the dynamics of oxygen ions (O^{2-}) as follows:

- formation of V_o by O^{2-} moving to an interstitial position;
- annihilation of V_o by moving O^{2-} to V_o.

To describe the motion of ions we have chosen the ion rates similar to (1):

$$\Gamma_n^{'} = A_i \cdot \frac{dE}{1-\exp\left(-dE/T\right)} \qquad (5)$$

Here we assume that O^{2-} can only move to the nearest interstitial. A distance-dependent term is thus included in A_i. dE includes the formation energy for the m-th V_o /annihilation energy of the m-th V_o, when O^{2-} is moving to an interstitial or back to V_o, respectively.

With the model supplemented by the motion of ions we simulated *I-V* characteristics. All calculations of the RRAM *I-V* characteristics are now performed on a two-dimensional lattice (2×30). We have investigated the *I-V* hysteresis by applying a saw-tooth-like voltage *V*. We have assumed that the coefficients of the boundary conditions are constant and equal to 0.1.

In the first moment of time we assume that there are no vacancies V_o. Each O^{2-} has a probability Γ'_n of moving to the nearest interstitial position (if this position is empty) making a formation of a new V_o possible; moreover, each O^{2-} has a probability Γ'_n of annihilation with the nearest V_o if this V_o is not occupied by an electron. In addition, the electron dynamics according to (1-3) on the vacancies V_o already formed must also be taken into account giving rise to the electron current in the system.

The simulated RRAM switching hysteresis cycle is

shown in Fig.4. The simulated cycle is in good agreement with the experimental cycle from [10] shown in the inset of Fig.4.

The interpretation of the RRAM hysteresis cycle obtained from the stochastic model is as follows. If a positive voltage is applied, the formation of a CF begins, when the voltage reaches a critical value sufficient to create V_o by moving O^{2-} to an interstitial position. The formation of the CF leads to a sharp increase in the current (Fig. 4 Segment 1) signifying a transition to a state with low resistance. When a reverse negative voltage is applied, the current increases linearly (Fig. 4 Segment 3), until the applied voltage reaches the value at which an annihilation of V_o is triggered by means of moving O^{2-} to V_o. The CF is ruptured and the current decreases (Fig. 4 Segment 4). This is the transition to a state with the high resistance.

IV. Conclusion

We have developed a stochastic model of the resistive switching mechanism. The results of our simulations are in excellent agreement with previous theoretical and experimental work. The distribution of the electron occupation probabilities calculated with the model is in excellent agreement with the mean-field results [19]. The simulated RRAM switching hysteresis cycle is in good agreement with the experimental data. The proposed stochastic model can be used for better understanding resistive switching in RRAM.

References

[1] B. C. Lee, P. Zhou, J. Yang, Y. T. Zhang, B. Zhao, E. Ipek, O. Mutlu, D. Burger, "Phase-Change Technology and the Future of Main Memory," IEEE Micro, vol. 30, no. 1, pp. 131-141, 2010.

[2] M. H. Kryder, C. S. Kim, "After Hard Drives - What Comes Next?," IEEE Trans. Magn., vol. 45, no. 10, pp. 3406-3413, 2009.

[3] C. Kugeler, C. Nauenheim, M. Meier, A. Rudiger, R. Waser, "Fast Resistance Switching of TiO2 and MSQ Thin Films for Non-Volatile Memory Applications (RRAM)," NVM Tech. Symp., p. 6, 2008.

[4] L. E. Yu, S. Kim, M. K. Ryu, S. Y. Choi, Y. K. Choi, "Structure Effects on Resistive Switching of Al/TiOx/Al Devices for RRAM Applications," IEEE Electron Device Lett., vol. 29, no. 4, pp. 331-333, 2008.

[5] D. S. Jeong, H. Schroeder, U. Breuer, R. Waser R, "Characteristic Electroforming Behavior in Pt/TiO2/Pt Resistive Switching Cells Depending on Atmosphere," J. Appl. Phys., vol. 104, no. 12, pp. 123716, 2008.

[6] H. Shima, N. Zhong, H. Akinaga, "Switchable Rectifier Built with Pt/TiOx/Pt Trilayer," Appl. Phys. Lett., vol. 94, no. 8, pp. 082905, 2009.

[7] Y. S. Chen, T. Y. Wu, P. J. Tzeng, "Forming-free HfO2 Bipolar RRAM Device with Improved Endurance and High Speed Operation," Symp. on VLSI Tech., pp. 37-38, 2009.

[8] R. Dong, D. S. Lee, W. F. Xiang, S. J. Oh, D. J. Seong, S. H. Heo, "Reproducible Hysteresis and Resistive Switching in Metal-CuxO-Metal Heterostructures," Appl. Phys. Lett., vol. 90, no. 4, pp. 42107/1-3, 2007.

[9] S. Seo, M. J. Lee, D. H Seo, S. K. Choi, D. S. Suh, Y. S. Joung, I. K. Yoo, I. S. Byun, I. R. Hwang, S. H. Kim, B. H. Park, "Conductivity Switching Characteristics and Reset Currents in NiO Films," Appl. Phys. Lett., vol. 86, no. 9, 2005.

[10] S. Lee, H. Kim, D. J. Yun, S. W. Rhee, K. Yong, "Resistive Switching Characteristics of ZnO Thin Film Grown on Stainless Steel for Flexible Nonvolatile Memory Devices," Appl. Phys. Lett., vol. 95, no. 26, pp. 262113, 2009.

[11] Y. Watanabe, J. G. Bednorz, A. Bietsch, Ch. Gerber, D. Widmer, A. Beck, and S. J. Wind, "Current-Driven Insulator–Conductor Transition and Nonvolatile Memory in Chromium-Doped SrTiO3 Single Crystals," Appl. Phys. Lett., vol. 78, no. 23, pp. 3738-3740, 2001.

[12] C. C. Lin, C. Y. Lin, M. H. Lin, "Voltage-Polarity-Independent and High-Speed Resistive Switching Properties of V-Doped SrZrO3 Thin Films," IEEE Trans. Electron Devices, vol. 54, no. 12, pp. 3146-3151, 2007.

[13] A. Sawa, T. Fujii, M. Kawasaki, and Y. Tokura, "Hysteretic Current–Voltage Characteristics and Resistance Switching at a Rectifying Ti/Pr0.7Ca0.3MnO3 Interface," Appl. Phys. Lett., vol. 85, no. 18, pp. 4073-4075, 2004.

[14] T. Fujii, M. Kawasaki, A. Sawa, H. Akoh, Y. Kawazoe, and Y. Tokura, "Hysteretic Current–Voltage Characteristics and Resistance Switching at an Epitaxial Oxide Schottky Junction SrRuO3/SrTi0.99Nb0.01O3," Appl. Phys. Lett., vol. 86, no. 1, art. no. 012107, 2005.

[15] Y. B. Nian, J. Strozier, N. J. Wu, X. Chen, A. Ignatiev, "Evidence for an Oxygen Diffusion Model for the Electric Pulse Induced Resistance Change Effect in Transition-Metal Oxides," PRL, vol. 98, no. 14, pp. 146403/1-4, 2007.

[16] S. X. Wu, L. M. Xu, X. J Xing, "Reverse-Bias-Induced Bipolar Resistance Switching in Pt/TiO2/SrTi0.99Nb0.01O3/Pt Devices," Appl. Phys. Lett., vol. 93, no. 4, pp. 043502/1-3, 2008.

[17] K. Szot, W. Speier, G. Bihlmayer and R. Waser, "Switching the Electrical Resistance of Individual Dislocations in Single-Crystalline SrTiO3," Nature Materials, vol. 5, pp. 312-320, 2006.

[18] Y. Nishi, J. R. Jameson, "Recent Progress in Resistance Change Memory," Dev. Res. Conf., pp. 271-274, 2008.

[19] B. Gao, B. Sun, H. Zhang, L. Liu, X. Liu, R. Han, J. Kang, B. Yu, "Unified Physical Model of Bipolar Oxide-Based Resistive Switching Memory," IEEE Electron Device Lett., vol. 30, no. 12, pp. 1326-1328, 2009.

[20] M. J. Rozenberg, I. H. Inoue, and M. J. Sanchez, "Nonvolatile Memory with Multilevel Switching: A Basic Model," PRL, vol. 92, no. 17, pp. 178302-1, 2004.

[21] K. Kinoshita, T. Tamura, H. Aso, H. Noshiro, C. Yoshida, M. Aoki, Y. Sugiyama, H. Tanaka, "New Model Proposed for Switching Mechanism of ReRAM," IEEE Non-Volatile Semicond. Memory Workshop, pp. 84 – 85, 2006.

[22] U. Russo, D. Ielmini, C. Cagli, A.L. Lacaita, S. Spiga, C. Wiemer, M. Perego, and M. Fanciulli, "Conductive-Filament Switching Analysis and Self-Accelerated Thermal Dissolution Model for Reset in NiO-Based RRAM," IEDM Tech. Dig., pp. 775-778, 2007.

[23] S. Kim, Y. K. Choi, "A Comprehensive Study of the Resistive Switching Mechanism in Al/TiOx/TiO2/Al-Structured RRAM," IEEE Trans. Electron Devices, vol. 56, no. 12, pp. 3049-3054, 2009.

[24] V. Sverdlov, A. N. Korotkov, K. K. Likharev, "Shot-Noise Suppression at Two-Dimensional Hopping," PRB, vol.63, 081302, 2001.

[25] C. Y. Lin, C. Y. Wu, C.-Y. Wu, T. C. Lee, F. L. Yang, C. Hu; T. Y. Tseng, "Effect of Top Electrode Material on Resistive Switching Properties of ZrO2 Film Memory Devices," IEEE Electron Device Lett., vol. 28, no. 5, pp. 366-8, 2007.

[26] W. G. Kim, S. W. Rhee, "Effect of the Top Electrode Material on the Resistive Switching of TiO2 Thin Film," Microelectronic Engineering, vol. 87, no. 2, pp. 98-103, 2010.